

3-26-1992

Scanning Electron Microscopy - Energy Dispersive Spectroscopy and X-Ray Diffraction Analyses of Human Salivary Stones

H. Mishima

Nihon University School of Dentistry at Matsudo

H. Yamamoto

Nihon University School of Dentistry at Matsudo

T. Sakae

Nihon University School of Dentistry at Matsudo

Follow this and additional works at: <https://digitalcommons.usu.edu/microscopy>



Part of the [Biology Commons](#)

Recommended Citation

Mishima, H.; Yamamoto, H.; and Sakae, T. (1992) "Scanning Electron Microscopy - Energy Dispersive Spectroscopy and X-Ray Diffraction Analyses of Human Salivary Stones," *Scanning Microscopy*: Vol. 6 : No. 2 , Article 14.

Available at: <https://digitalcommons.usu.edu/microscopy/vol6/iss2/14>

This Article is brought to you for free and open access by the Western Dairy Center at DigitalCommons@USU. It has been accepted for inclusion in Scanning Microscopy by an authorized administrator of DigitalCommons@USU. For more information, please contact digitalcommons@usu.edu.



SCANNING ELECTRON MICROSCOPY - ENERGY DISPERSIVE SPECTROSCOPY AND X-RAY DIFFRACTION ANALYSES OF HUMAN SALIVARY STONES

H. Mishima^{1*}, H. Yamamoto² and T. Sakae¹

¹Department of Anatomy and ²Pathology,
Nihon University School of Dentistry at Matsudo, Chiba 271, Japan

(Received for publication January 13, 1992, and in revised form March 26, 1992)

Abstract

Ten salivary stones in the human submandibular gland were investigated by scanning electron microscopy-energy dispersive spectroscopy (SEM-EDS) and X-ray diffraction analyses. The stones usually showed a lamellar pattern. SEM observations revealed cubical, plate-like, granular, small and large granules, polyhedral or globular structures in these stones. By X-ray powder diffraction analysis, the main constituents of salivary stones were found to be apatite and whitlockite. SEM-EDS analyses showed that Ca and P were the major elements, frequently accompanied by Mg and S, and less frequently by Na, Al, Si, Cl, K, Fe, Cu and Zn. Ca/P molar ratios ranged from 1.00 to 2.00 with the average of 1.53, showing two maxima of about 1.50 and 1.60. The Ca/P molar ratio of about 1.50 corresponded to the value of whitlockite. The Ca/P molar ratio of 1.60 corresponded approximately to the value of apatite.

Key Words: Salivary stone, scanning electron microscopy, energy dispersive spectroscopy, X-ray diffraction, hydroxyapatite, whitlockite.

*Address for correspondence:

H. Mishima
Department of Anatomy,
Nihon University School of Dentistry at Matsudo,
2-870-1 Sakaecho-Nishi,
Matsudo, Chiba 271,
Japan

Phone No.: 0473-68-6111 Ext. 386

Introduction

Salivary gland stones generally form within the duct of exocrine glands [5]. These stones consist of organic and inorganic components, and are assumed to grow by the rhythmic deposition of alternating layers of organic and inorganic substances around a central nucleus [3]. Burstein *et al.* [5] have shown that hydroxyapatite (HA) occurs most frequently in salivary stones with a small amount of magnesium-substituted whitlockite.

Salivary stones have been studied by X-ray crystallographical analysis [3, 11, 12, 20, 21], chemical analysis [1, 2, 4, 6, 7, 10, 17, 18] or both techniques [5, 19]. However, studies using both techniques have not been applied extensively and conclusively. The purpose of this study is to investigate the mineral composition of salivary stones by a combination of scanning electron microscopy-energy dispersive X-ray microanalysis (SEM-EDS) and X-ray diffraction analysis.

Materials and Methods

Ten salivary stones were collected from the human submandibular gland of 7 male patients and 3 female patients at the Dental Hospital of Nihon University School of Dentistry at Matsudo. The patients' age ranged from 12 to 58. The samples were stored in 10 % neutral formaldehyde solution for 24 h. After rinsing with distilled water, they were divided into two pieces and processed as follows:

One half of the stones was dehydrated in a series of ethanol, and dried in air. They were pulverized in an agate mortar. X-ray diffraction analysis was carried out on the powder by a X-ray diffractometer (RIGAKU, Tokyo) under the following conditions: X-ray tube voltage, 40 kV; tube current, 20 mA; Cu target; Ni filter (wavelength, 0.15418 nm); slit system, 1°-0.3 mm⁻¹; scan speed, 1 degree/min. (2 θ); time constant, 2.

The other half was dehydrated in a series of ethanol, substituted with isoamyl acetate, and subjected to critical-point drying with carbon dioxide. The surface was carbon-coated in a TB-500 carbon coater (EMSCOPE

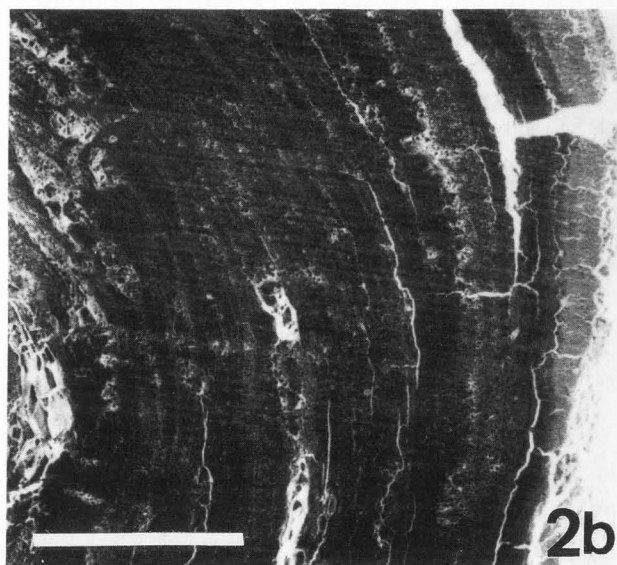
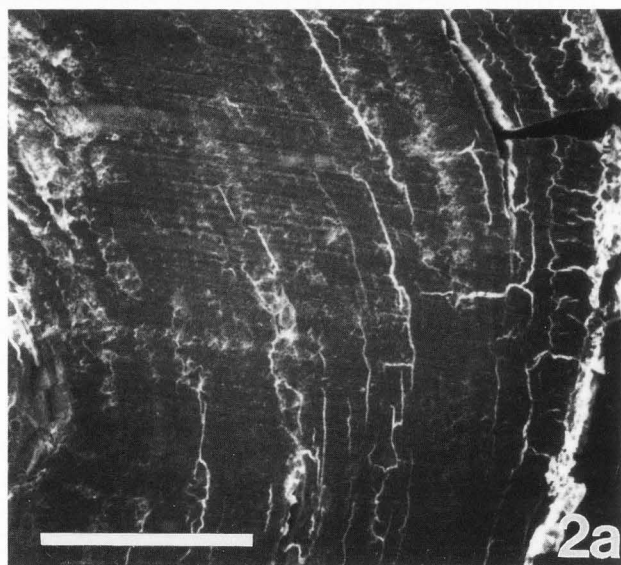
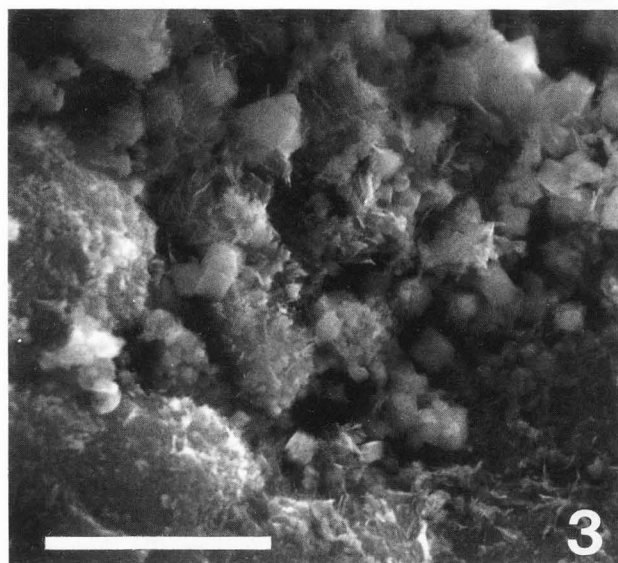
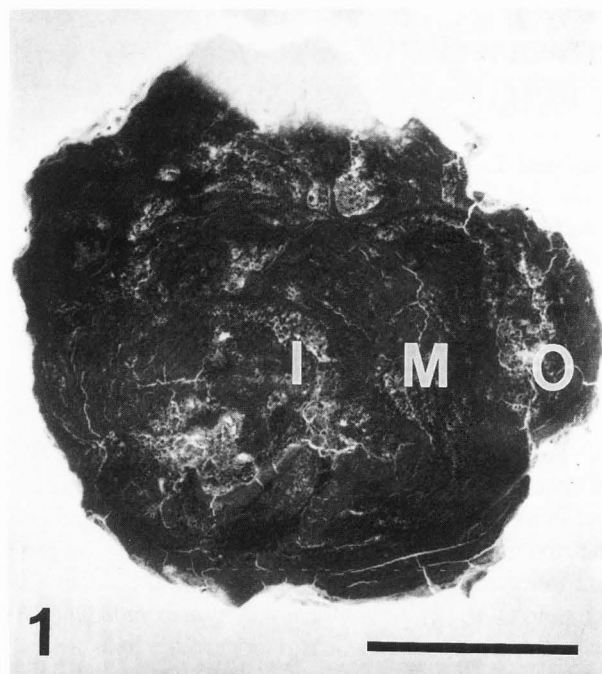


Figure 1. Backscattered electron image of a ground section of a salivary stone. The sample could be divided into the inner layer (I), the middle layer (M), and the outer layer (O). Bar = 1.2 mm.

Figure 2. (a) Secondary and (b) backscattered electron images of a ground section of a salivary stone. In (a) the structure of the salivary stone shows a lamellar pattern, which is clearly visualized in (b). Bar = 1 mm.

Figure 3. Secondary electron image of a salivary stone. Small cubical (label) and plate-like (label) structures were observed in the nucleus of the inner layer. Bar = 10 μ m.

Laboratories, Ltd.) for scanning electron microscopic (SEM) observation and energy dispersive X-ray microanalysis (EDS). The estimated thickness of the carbon coat was about 50 nm. SEM observations were carried

out by both the secondary and backscattered electron imaging techniques using a JSM T200 (JEOL, Tokyo) and a S-2500 Δ (HITACHI) with an accelerating voltage of 25 kV and working distance of 20 mm. EDS analysis

Analysis of Salivary Stones

Table 1. Elements present in salivary stone.

Location	Structure	Elements
Outer layer	Granular structure	Mg, P, S, Ca
Outer layer	Polyhedral crystals	P, S, Ca, Fe
Outer layer	Plate-like crystals	P, Ca
Middle layer	Small granules	Mg, Al, P, Ca
Inner layer	Large granules	Al, P, Ca
Inner layer	Cubical crystals	Mg, Si, P, Ca
Inner layer	Globular structure	P, S, Ca

was carried out by point-mode with a JED-2000 (JEOL, Tokyo) attached to the T200 under the following conditions: X-tilt angle, 30°; take-off angle, 41.18°; counting time, 100 seconds. About 10 points were analyzed on one sample. The total amount of point analyses was 107. The atomic percentages of the different elements were calculated using an AUTO-ZAP program assuming the total weight per cent of cationic atoms being 100. The Ca/P values were expressed as molar ratios. Some specimens were cut and ground into a thin sections 100 μm thick. These sections were examined by a SEM.

Results

Figure 1 shows a backscattered SEM image of a ground section of a salivary stone. All samples demonstrated the inner layer (I), the middle layer (M), and the outer layer (O). Each layer usually showed a lamellar pattern (Fig. 2a). Backscattered electron images (Fig. 2b) showed the lamellar pattern more clearly than the secondary electron image (Fig. 2a). In the nucleus of the inner layer, small cubical or plate-like structures were observed (Fig. 3).

X-ray powder diffraction showed that the main constituents were apatite and whitlockite (Fig. 4). The asterisks show the peaks of whitlockite. These salivary stones did not show peaks of any other crystalline calcium phosphates.

Figure 5 shows granular structures in the outer layer of a stone. EDS analysis demonstrated that the structures had major peaks of Ca and P, and minor peaks of Mg and S (Table 1). The Ca/P molar ratio was 1.46. Figure 6 shows polyhedral crystals in the outer layer. EDS analysis of these crystals demonstrated that Ca and P were the major elements, but small amounts of S and Fe were also detected (Table 1). The Ca/P molar ratio was 1.54. Figure 7 shows plate-like crystals in the outer layer. By EDS analysis, Ca and P could be detected (Table 1). The Ca/P molar ratio was 1.66 very close to the value of hydroxyapatite. Figure 8 shows small granules in the middle layer. EDS analysis of these granules showed that Ca and P were the major elements. Mg and

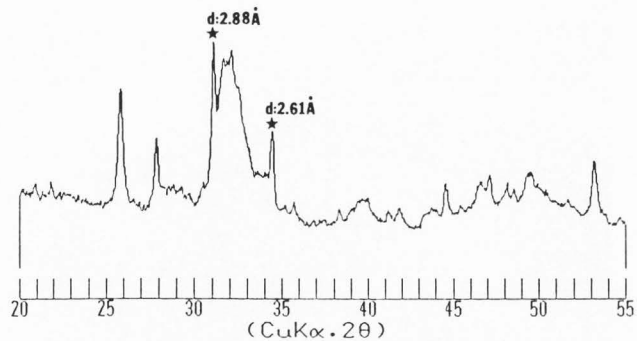


Figure 4. X-ray diffraction pattern of a salivary stone. Asterisks show the peak of whitlockite. The other peaks show the peak of apatite. The axis abscissa represents the diffraction angle in 2θ degrees.

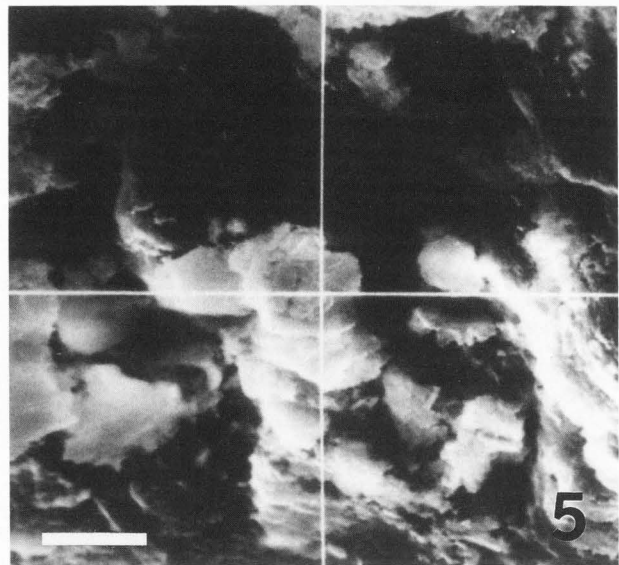


Figure 5. A secondary electron image of the granular structures (label) in the outer layer. The crossing is the measurement point. Bar = 10 μm .

Al were also detected in small amounts (Table 1). The Ca/P molar ratio was 1.41. Figure 9 shows large granules in the inner layer. By EDS analysis, the major peaks were Ca and P, and Al was also detected in low amounts (Table 1). The Ca/P molar ratio was 1.42. Figure 10 shows cubical crystals in the inner layer. By EDS analysis, the major peaks were Ca and P. As compared with the outer and middle layers of the sample, Mg and Si were detected in low amounts (Table 1). The Ca/P molar ratio was 1.61. Globular structures were observed in the inner layer (Fig. 11). EDS analysis of the globular structure showed that the major peaks were Ca and P, and S was also detected in small amounts (Table 1). The Ca/P molar ratio was 1.52.

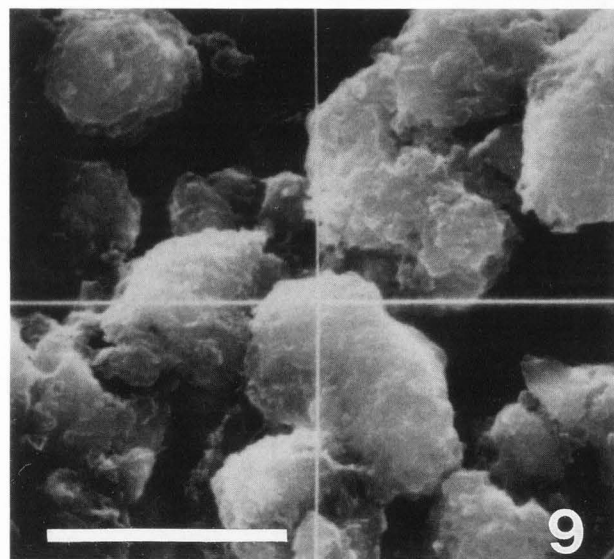
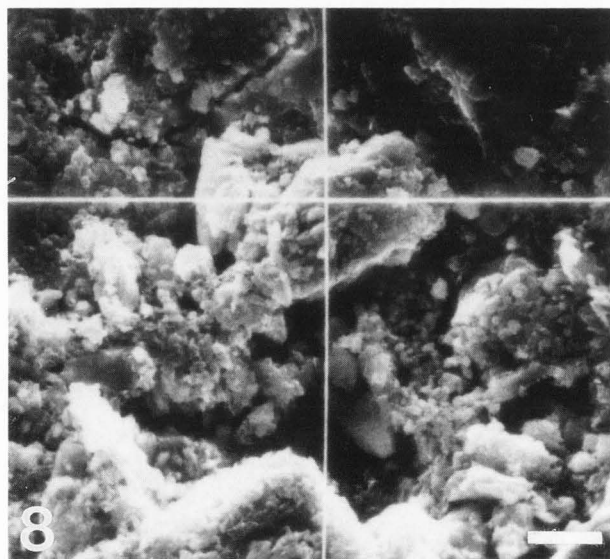
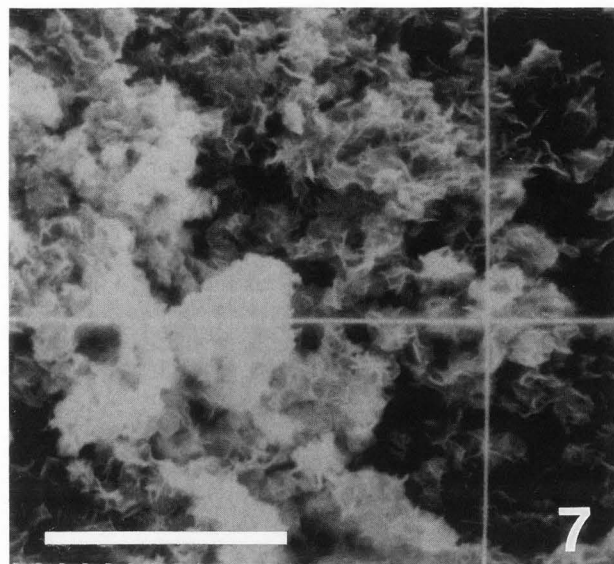
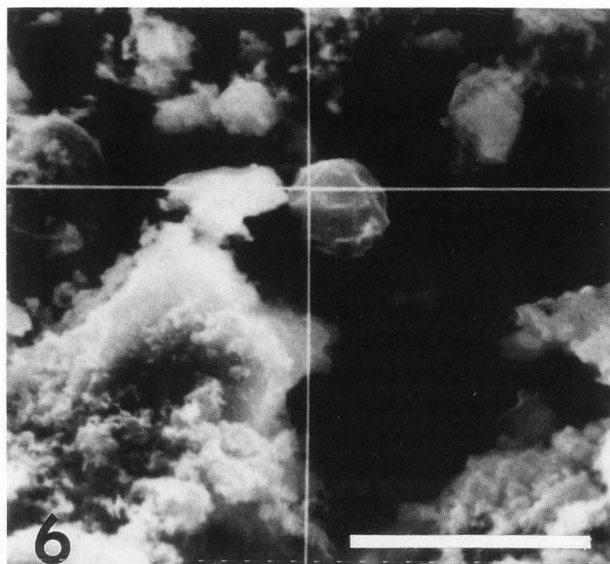


Figure 6. A secondary electron image of the polyhedral crystals (label) in the outer layer. Bar = 10 μm .

Figure 7. A secondary electron image of the plate-like crystals (label) in the outer layer. Bar = 10 μm .

Figure 8. A secondary electron image of the small granules (label) in the middle layer. Bar = 10 μm .

Figure 9. A secondary electron image of the large granules (label) in the inner layer. Bar = 10 μm .

Figure 12 shows the frequency distribution of the values of the Ca/P molar ratios. The values ranged from 1.00 to 2.00 with the average of 1.53. The ratios showed two maxima of about 1.50 and 1.60. Figure 13 shows occurrence of various elements from the samples

detected by EDS. Ca and P (100%) were always present, and Na, K, Mg, Al, Si, S, Cl, Fe, Cu, and Zn occurred infrequently. S (53%) and Mg (27%) were present more frequently than the other minor elements.

Analysis of Salivary Stones

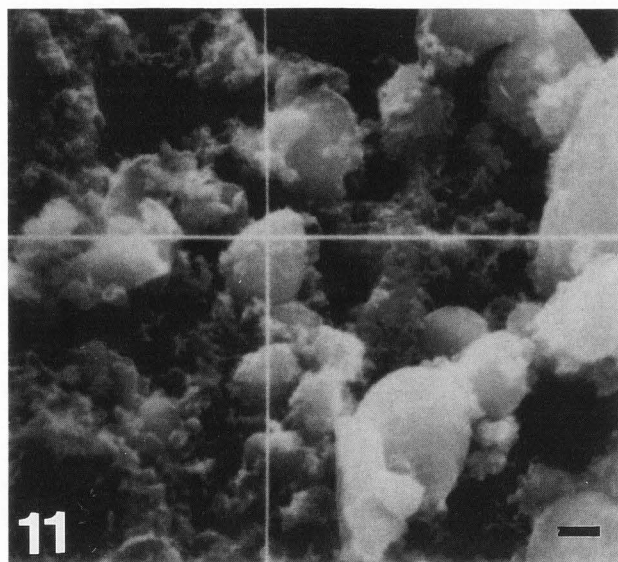
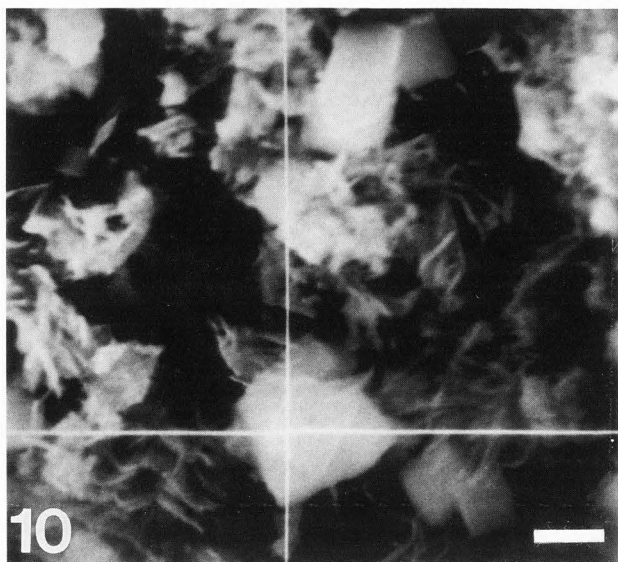


Figure 10. A secondary electron image of the cubical crystal (label) in the inner layer. Bar = 1 μm .

Figure 11. A secondary electron image of the globular structure (label) in the inner layer. Bar = 1 μm .

Discussion

Backscattered electron images of salivary stones showed a lamellar pattern. Cubical, plate-like, granular, small and large granules, polyhedral or globular structures were observed. X-ray diffraction analysis demonstrated that the main constituents of salivary stones were

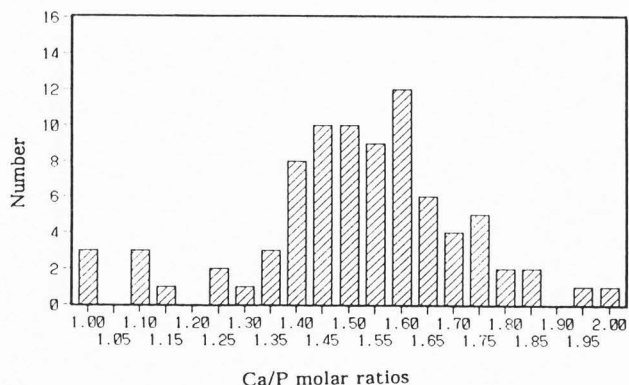


Figure 12. Distribution of the different Ca/P molar ratios. The number of analyzed points is 83. The points below 1.00 or above 2.00 have been excluded.

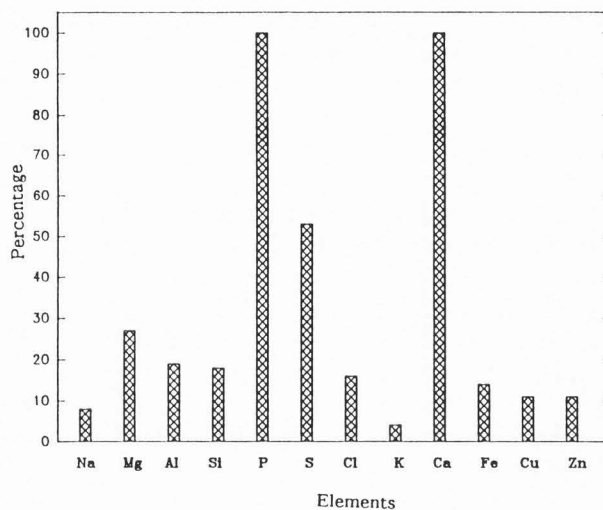


Figure 13. Bar graph of the elements detected by EDS. Percentage shows the occurrence of element. The total number of analyzed points is 107.

apatite and whitlockite. By SEM-EDS analysis, it was found that Ca and P were the major elements, while other elements such as Na, Mg, Al, Si, S, Cl, K, Fe, Cu and Zn were also detected. Sulphur and magnesium often could be detected. The Ca/P molar ratios showed two maxima of about 1.50 and 1.60.

Hydroxyapatite, octacalcium phosphate (OCP), whitlockite (β -TCMP), brushite, weddellite and calcite have been reported as the crystalline phase of salivary stones [3, 5, 11-14, 20, 21]. Hydroxyapatite and Mg-substituted whitlockite are generally accepted as co-phases in salivary stones of submandibular origin [5]. Vignoles *et al.* [19] have reported that the salivary calculi were composed of a nucleus and a shell which contain an organic phase with two crystalline mineral

phases, whitlockite and apatite. Yamamoto *et al.* [21] have demonstrated that apatite was frequently observed and that whitlockite was next frequently detected in the calculi. Our results agree with the findings of Burstein *et al.* [5], Vignoles *et al.* [19] and Yamamoto *et al.* [21] that the salivary stones consist of hydroxyapatite and whitlockite. It is suggested that OCP, brushite, weddellite and calcite are rarely present in the salivary stones.

The Ca/P molar ratios ranged from 1.00 to 2.00 with the average of 1.53 in the salivary stones analyzed. Most samples had ratios of 1.50 or 1.60. LeGeros *et al.* [8] showed, by electron microprobe analysis, that the crystalline components of dental calculi had Ca/P ratios close to 1.3 (OCP), close to 1.4 (β -TCMP), and close to 1.7 (CHA or CO₃-substituted apatite). By our EDS analysis, the Ca/P molar ratio of whitlockite showed 1.49 [15] and the Ca/P molar ratio of synthetic apatite showed 1.60 [9]. The Ca/P molar ratio of about 1.50 obtained in the present study correspond to the value of whitlockite. In addition, the Ca/P molar ratio of approximately 1.60 corresponds to the value of apatite. These results are in agreement with X-ray diffraction data.

The earlier elemental electron microprobe analyses showed the presence of F, Na, Mg, Al, Si, P, S, Cl, K, Ca, Fe, Cu and Zn in the salivary calculi [2, 4, 6, 7, 10, 16-18]. Our energy dispersive X-ray microanalyses have shown that sulphur and magnesium could be detected frequently besides the main components Ca and P. Faure *et al.* [6] reported that inclusions with high silicon or sulphur concentrations were found in all 8 samples. Sulphur was frequently detected in the salivary stones [2, 4, 7, 17, 18]. Tanda *et al.* [17] have suggested that sulphur may be present in salivary proteins and exfoliated epithelial cells. Sulphur is probably present as sulphated proteoglycans and has some function in the formation of salivary stones. Meanwhile, it was clarified that Mg is principally associated with the β -TCMP component [8]. We conclude that the presence of magnesium ions in the salivary stone supports the idea that magnesium ions induce whitlockite formation.

Fe may originate from the blood. Na and K may come from the extracellular or intercellular fluids. Al, Si, Cl, Cu and Zn may come from the denture or filling in the oral cavity. These elements are not artifacts generated in the microscope column, because analysis of synthetic monetite did not show these elements.

Acknowledgements

A portion of this work was supported by the funds of Electron Microscopy Center, University of South Carolina. We would like to thank the staff of the Department of Anatomy, Nihon University School of

Dentistry at Matsudo, for their instruction and assistance, Professor Dr. N. Watabe of University of South Carolina, for reviewing the manuscript and Professor Dr. H.-J. Höhling of the Universität Münster, for helpful discussions.

References

1. Akahane S, Eda S, Kawakami T, Nakamura C, Hasegawa H, Yoshida J, Chino T (1986). Ultrastructural studies on the salivary calculus. First report: calcification in filamentous microorganisms, *Matsumoto Shigaku* **12**: 189-201.
2. Akaiwa Y, Ando Y, Hino T, Kurisaki Y, Fujii K, Hashimoto H (1985). A methodological study on the analysis of X-ray images from the electron microprobe X-ray analyzer (2) - Compositional zoning of human salivary calculus by computer-aided micro analyzer (CMA), *Bull Josai Dent Univ* **14**: 88-91.
3. Anneroth G, Eneroth CM, Isacson G (1975). Crystalline structure of salivary calculi. A micro-radiographic and microdiffractometric study, *J Oral Pathol* **4**: 266-272.
4. Azuma T (1973). Electron microprobe analysis of salivary calculus, *Odontology* **61**: 124-164.
5. Burstein LS, Boskey AL, Tannenbaum PJ, Posner AS, Mandel ID (1979). The crystal chemistry of submandibular and parotid salivary gland stones, *J Oral Pathol* **8**: 284-291.
6. Faure J, Vignoles M, Bonel G, Lodter JPh (1986). Microanalyse des calculs salivaires, *J Biol Buccale* **14**: 195-205.
7. Kitagawa H (1988). Microstructural and elemental analyses on cross sections of sialolith, *Kurume Med J* **51**: 762-782.
8. LeGeros RZ, Orly I, LeGeros JP, Gomez C, Kazimiroff J, Tarpley T, Kerebel B (1988). Scanning electron microscopy and electron probe microanalyses of the crystalline components of human and animal dental calculi, *Scanning Microsc* **2**: 345-356.
9. Mishima H, Sakae T, Kozawa Y, Yamamoto H, Numata T, Hirai G (1989). Energy Dispersive X-ray Analysis of Human Deciduous Teeth Dentin, *Nihon Univ J oral Sci* **15**: 43-46.
10. Miyake M, Ishi T, Andoh M, Takayama Y, Tohyama Y, Hori M, Fujisaki T, Asahina H, Tanaka H, Sato H (1987). Submandibular gland sialolithiasis - Sialographic and pathologic findings with evaluation using SEM and EPMA analysis, *J Nihon Univ Sch Dent* **29**: 112-123.
11. Sakae T, Hirai G, Yamamoto H (1979). X-ray diffraction patterns of apatite in enamel, dentine, cement, bone, and salivary stone with X-ray microdiffractometer, *Nihon Univ J oral Sci* **5**: 206-210.

12. Sakae T, Yamamoto H, Hirai G (1981). Mode of occurrence of brushite and whitlockite in a sialolith, *J Dent Res* **60**: 842-844.

13. Sakae T, Yamamoto H, Mishima H, Okuda A, Ishii S, Hirai G (1982). Identification of hard tissue crystals by X-ray diffraction method, *Nihon Univ J oral Sci* **8**: 399-407.

14. Sakae T, Yamamoto H, Okuda A (1984). Scanning electron microscopic observation of crystal habits of weddellite from a sialolith, *Nihon Univ J oral Sci* **10**: 84-86.

15. Sakae T, Yamamoto H, Mishima H, Matsumoto T, Kozawa Y (1989). Morphology and chemical composition of dental calculi mainly composed of whitlockite, *Scanning Microsc* **3**: 855-860.

16. Taen A, Kodama K (1972). Ten cases of sialolithiasis in the past of three years, *Jpn J Oral Maxillofac Surg* **18**: 341-346.

17. Takeda Y (1986). Crystalloids with calcareous deposition in the parotid gland: one of the possible causes of development of salivary calculi, *J Oral Pathol* **15**: 459-461.

18. Tanda N, Echigo S, Teshima T (1988). Sialolithiasis of a Blandin's gland duct, *Int J Oral Maxillofac Surg* **17**: 78-80.

19. Vignoles M, Faure J, Legros R, Bonel G, Guichard M (1980). Contribution à l'identification du constituant minéral de quelques calculs salivaires par l'étude de leur comportement thermique, *J Biol Buccale* **8**: 103-115.

20. Yamamoto H, Sakae T, Takagi M, Otake S, Hirai G (1983). Weddellite in submandibular gland calculus, *J Dent Res* **62**: 16-19.

21. Yamamoto H, Sakae T, Takagi M, Otake S (1984). Scanning electron microscopic and X-ray micro-diffractometric studies on sialolith-crystals in human submandibular glands, *Acta Pathol Jpn* **34**: 47-53.

Discussion with Reviewers

S.H. Ashrafi: How much does your study differ from Burstein *et al.* (1979), Vignoles *et al.* and Yamamoto *et al.* (1984)?

Authors: By SEM-EDS analysis, it was found that Ca and P were the major elements, while other elements such as Na, Mg, Al, Si, S, Cl, K, Fe, Cu and Zn were also detected. S and Mg were often detected. Ca/P molar ratios ranged from 1.00 to 2.00 with the average of 1.53, showing two maxima of about 1.50 and 1.60. The Ca/P molar ratio of about 1.50 obtained in the present study corresponded to the value of whitlockite. The Ca/P molar ratio of about 1.60 corresponded to the value of apatite.

A.L. Boskey: Please describe briefly how this study has expanded our knowledge of human salivary stones.

Authors: The SEM-EDS analysis in this study showed that Mg and S could be detected frequently besides the main components Ca and P. The Ca/P molar ratios had two maxima of about 1.50 and 1.60. Salivary stones are principally constituted of apatite and whitlockite.

A.L. Boskey: Considering all reports of stones analyzed, (your 10 plus all of those cited), what is the relative distribution of the different mineral phases? Based on these numbers, rather than on the 10 in your study, can you conclude that HA and whitlockite are most often found in human salivary stones?

Authors: Our study showed the salivary stones consisted of apatite and whitlockite. The biological apatite is similar to hydroxyapatite. The X-ray diffraction pattern shown here was not identified as hydroxyapatite, but was only identified as apatite. We conclude that apatite was frequently observed and that whitlockite was next frequently detected in human salivary stones. Apatite was observed in both outside and inside of the salivary stones [21]. Whitlockite was seen more often in the central regions of salivary stones [3, 5, 21].

O. Le May: Since others compounds such as octacalcium phosphate, brushite, calcite and weddellite have been evidenced by other studies, how do you explain that you only identify hydroxyapatite and whitlockite in the present study?

Authors: We think that the major components of the crystalline phase of submandibular gland salivary stones are apatite and whitlockite. We estimated that octacalcium phosphate, brushite, weddellite and calcite are rarely present in the salivary stones. It is suggested that brushite and weddellite were present in the front portion of calculus formation and then transformed into the more stable form e.g., apatite [21]. It is possible that the lower pH of the parotid saliva acts to stabilize the octacalcium phase while the higher pH of the submandibular gland allows for transformation of octacalcium phosphate to hydroxyapatite [5].

O. Le May: Since the salivary stones present a lamellar pattern around a nucleus, have you detected differences in the element concentrations in this nucleus compared to the other layers?

Authors: In one case, Mg and Si were localized in the nucleus compared to the middle and outer layer. In the other cases, we have not detected differences in the elemental concentrations.

G.M. Roomans: In your quantitative analysis, you assume that the sum of all cations adds up to 100%. This

does not take into account that a large part of the stone consists of oxygen. This must affect the absorption correction in the ZAP program. Do you think that it affects the calculated Ca:P ratio?

Authors: Yes, we think that it affects the calculate Ca:P ratio. It is considered that the frequency distribution of the values of the Ca/P molar ratios was influenced by oxygen.